Synthesis of Pyrroloquinolinequinone Analogs. Molecular Structure and Mössbauer and Magnetic Properties of Their Iron Complexes

L. Tommasi,[†] L. Shechter-Barloy,[‡] D. Varech,[‡] J.-P. Battioni,[‡,§] B. Donnadieu,[†] M. Verelst,[†] A. Bousseksou,[†] D. Mansuy,*[,‡] and J.-P. Tuchagues*[,†]

Laboratoire de Chimie de Coordination du CNRS, UP 8241 liée par conventions à l'Université Paul Sabatier et à l'Institut National Polytechnique, 205 route de Narbonne, 31077 Toulouse Cedex, France, and Laboratoire de Chimie et Biochimie Pharmacologiques et Toxicologiques, URA 400, Université René Descartes, 45 rue des Saints-Pères, 75270 Paris Cedex 06, France

Received November 8, 1994[⊗]

Four complexes, $Fe^{II}(L^2)_2$ (**1**), $[Fe^{II}(L^2)(Cl)(MeOH)_2]_2$ (**2**), $Fe^{II}(L^3H_2)_2$ (**3**), and $Fe^{III}(L^4)_2Cl{\cdot}2(Et_3N{\cdot}HCl){\cdot}0.5CH_3CN$ (**4**), wherein L^2H, L^3H_3, and L^4H are analogs of pyrroloquinolinequinone or methoxatin (PQQ), have been synthesized and studied. **2** crystallizes in the triclinic system, space group $P\bar{1}$, $Z = 2$, $a = 9.588(6)$ Å, $b = 10.011(7)$ Å, $c = 11.770(5)$ Å, $\alpha = 96.66(5)°$, $\beta = 99.21(5)°$, and $\gamma = 107.93(7)°$. The structure was solved by direct methods and refined to conventional agreement indices $R = 0.054$ and $R_w = 0.063$ with 2683 unique reflections for which $I > 3\sigma(I)$. The molecular structure of **2** consists of discrete $[Fe^{II}(L^2)(Cl)(MeOH)_2]$ molecules associated into dimeric units through the carboxylate function of L^2. The carboxylate oxygen atoms of the two molecules constituting the dimeric unit bridge the metal centers affording a Fe···Fe′ separation of 3.645(4) Å. The distorted coordination octahedron around each Fe(II) includes the pyridine nitrogen and carboxylate oxygen atoms of L^2, the chloride anion, and the oxygen atom of two methanol molecules. The synthesis and IR, Mössbauer, and magnetic susceptibility studies of **1**−**4** evidence the variety of structural types and nuclearities obtained for iron complexes of PQQ analogs, depending upon the stoichiometry and pH of the reactions. Complexes **1** and **3** (mononuclear) and **4** (polynuclear) are characterized by the 1:2 Fe:L ratio while complex **2** (dimer) is characterized by the 1:1 Fe:L ratio. Among the analogs used in this study, those of the reduced form of PQQ chelate iron through their tridentate site while chelation occurs preferentially at the quinonic site for the analog of the oxidized form of PQQ.

Introduction

2,7,9-Tricarboxy-1*H*-pyrrolo[2,3-*f*]quinoline-4,5-dione (usually named pyrroloquinolinequinone or methoxatin and abbreviated PQQ, Figure 1) is involved as cofactor in enzymes of the quinoproteins group.[1] Bacterial, NAD(P)-independent, periplasmic dehydrogenases involved in the oxidation of alcohols and aldose sugars belong to this group of enzymes, and the overall behavior of quinoprotein dehydrogenases is similar to that of dehydrogenases using a flavin cofactor or a nicotinamide coenzyme. Although it is clear that PQQ occurs in dehydrogenases of Gram-negative bacteria, its presence in other organisms like plants and animals is controversial.[2] Furthermore, the occurrence of covalently bound PQQ has been dismissed for several enzymes previously considered to contain this prosthetic group.[3]

The discovery of this quinonoid cofactor in metalloenzymes suggests that research on the interplay between the inorganic and organic cofactors could resolve long-standing problems on the mechanism of action for several of these enzymes.[1] The carboxylic acid groups of PQQ seem essential for binding in glucose dehydrogenase and methanol dehydrogenase,[4] and since Ca (Mg) is essential in reconstitution with PQQ of apoenzymes,

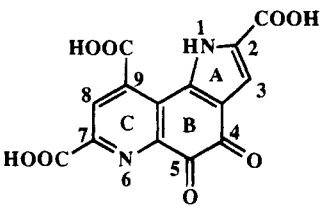

Figure 1. Schematic drawing of the pyrroloquinolinequinone cofactor (PQQ) with conventional atom numbering.

it has been proposed that the metal ions form a bridge between the carboxylic acid group(s) of PQQ and amino-acid residues in the protein. Moreover, reconstitution studies have shown that the active holoenzyme can be formed from the apoenzyme of glucose dehydrogenase in the presence of PQQ and other divalent cations with similar ionic radii.[5] Recently, by using Ca complexes of 2,7- and 2,9-dimethyl ester derivatives of PQQ,

* To whom correspondence should be addressed.
† Laboratoire de Chimie de Coordination.
‡ Laboratoire de Chimie et Biochimie Pharmacologiques et Toxicologiques.
§ Deceased.
⊗ Abstract published in *Advance ACS Abstracts,* February 15, 1995.

(1) Duine, J. A. *Eur. J. Biochem.* **1991**, *200,* 271.
(2) (a) Van der Meer, R. A.; Groen, B. W.; Jongejan, J. A.; Duine, J. A. *FEBS Lett.* **1990**, *251,* 131. (b) Van der Meer, R. A.; Groen, B. W.; Jongejan, J. A.; Duine, J. A. *FEBS Lett.* **1990**, *254,* 254.
(3) (a) Duine, J. A.; Frank, J.; Verwiel, P. E. J. *Eur. J. Biochem.* **1981**, *118,* 395. (b) Groen, B. W.; Frank, J.; Duine, J. A. *Biochem. J.* **1984**, *223,* 921. (c) Groen, B. W.; Van Kleef, M. A. G.; Duine, J. A. *Biochem. J.* **1986**, *234,* 611. (d) Adachi, O.; Shinagawa, E.; Matsushita, K.; Ameyama, M. *Agric. Biol. Chem.* **1982**, *46,* 2859. (e) Duine, J. A.; Frank, J.; Van Zeeland, J. K. *FEBS Lett.* **1979**, *108,* 443. (f) Hommes, R. W. J.; Postma, P. W.; Neijssel, O. M.; Tempest, D. W.; Dokter, P.; Duine, J. A. *FEMS Microbiol. Lett.* **1984**, *24* , 329. (g) Van Kleef, M. A. G.; Duine, J. A. *Arch. Microbiol.* **1988**, *150,* 32. (h) Shimao, M.; Yamamoto, H.; Ninomiya, K.; Kato, N.; Adachi, O.; Ameyama, M. *Agric. Biol. Chem.* **1984**, *48,* 2873.
(4) (a) Shinagawa, E.; Matsushita, K.; Nonobe, M.; Adachi, O.; Ameyama, M.; Ohsiro, Y.; Itoh, S.; Kitamura, Y. *Biochem. Biophys. Res. Commun.* **1985**, *139,* 1279. (b) Conlin, M.; Forrest, H. S.; Bruice, T. C. *Biochem. Biophys. Res. Commun.* **1985**, *131,* 554.
(5) Geiger, O.; Görisch, H. *J. Biochem.* **1989**, *261,* 415.

0020-1669/95/1334-1514$09.00/0

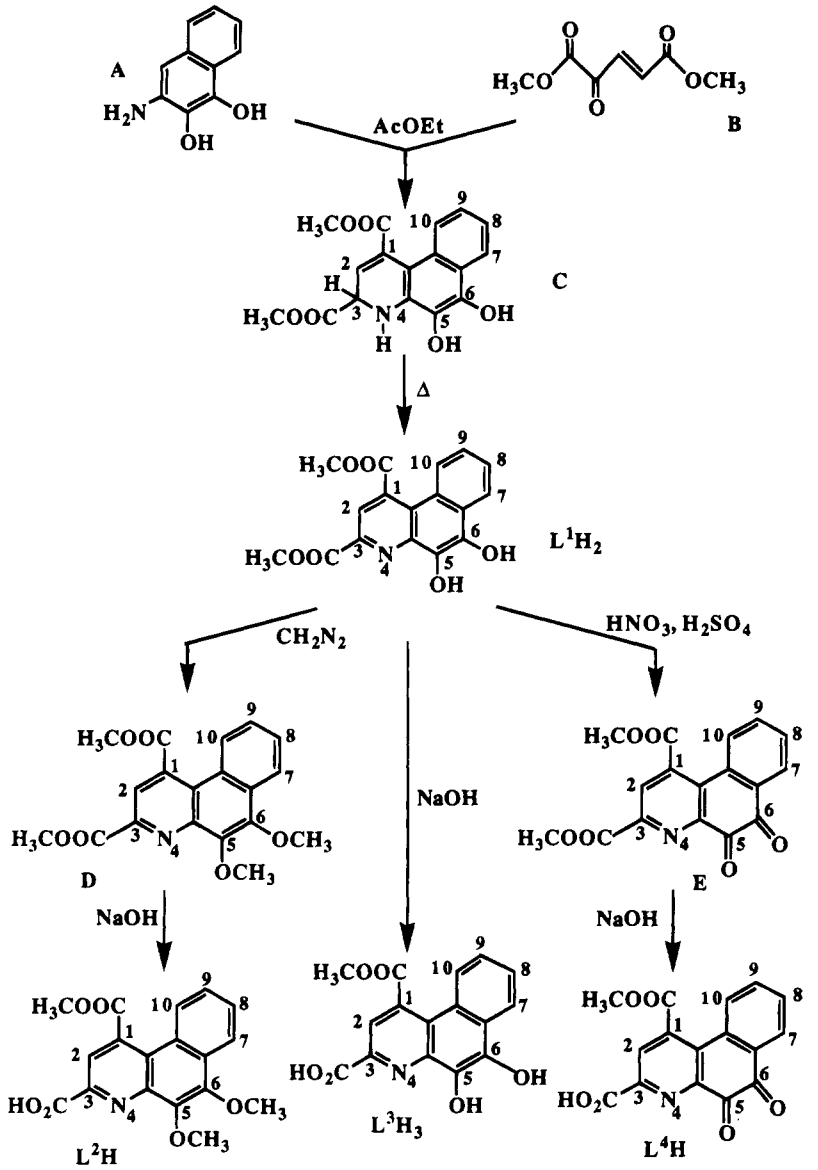

Figure 2. Schematic drawing of the synthetic route to the PQQ analogs L^1H_2, L^2H, L^3H_3, and L^4H.

Itoh *et al.* have shown that coordination of Ca to the pyridine and quinone functions is essential for efficient alcohol oxidation in vitro.[6]

PQQ may provide several binding sites for transition metal ions, and the 4,5-orthoquinone, 6-pyridine, and 7-carboxylic acid functions appear of great importance in this regard.[6,7] Some iron-containing enzymes have been proposed to include a PQQ moiety.[8] However, it has been recently established that the iron of the active site of lipoxygenase is not bound to PQQ,[9] and this possibility has been jeopardized in the case of nitrile hydratase.[10] In order to explore the role of the quinone (or catechol), pyridine, and carboxylic acid functions of PQQ in the chelation of metal ions, we have synthesized various analogs of PQQ such as L^4H and L^3H_3 which contain these three potential binding sites, L^1H_2, where the 3-COOH site has been esterified, and L^2H, where the catechol OH groups have been methylated (Figure 2). We have then studied their reactions with iron salts. The resulting complexes are interesting as models of possible iron–quinoproteins. Moreover, the choice of iron(II) to study the interaction of a divalent cation with PQQ analogs resulted also from the following considerations: (i) Fe^{2+} has an ionic radius close to that of Ca^{2+} and can be directly studied by Mössbauer spectrometry, a powerful technique which allows a detailed analysis of the electronic and structural properties of its ligand environment and (ii) it is redox active. Consequently, comparison of the complexes afforded by its reaction with either the catechol or quinone form of PQQ analogs could help understand the suspected relationship between coordination of a metal ion at the quinone site and specific redox activity of this quinonoid cofactor which may

(6) Itoh, S.; Huang, X.; Murao, H.; Komatsu, M.; Ohshiro, Y. Presented at the *6th Int. Conf. Bioinorg. Chem.*, San Diego, CA, *Aug 23–27*, 1993; *J. Inorg. Biochem.* **1993**, *51*, 87.

(7) (a) Nakamura, N.; Kohzuma, T.; Kuma, H.; Suzuki, S. *Acta Crystallogr. C* **1993**, *49*, 2093. (b) Ishida, T.; Doi, M.; Tomita, K.; Hayashi, H.; Inoue, M.; Urakami, Y. *J. Am. Chem. Soc.* **1989**, *111*, 6822. (c) Suzuki, S.; Sakurai, T.; Ohshiro, Y. *Inorg. Chem.* **1988**, *27*, 591. (d) Noar, J. B.; Rodriguez, E. J.; Bruice, T. C. *J. Am. Chem. Soc.* **1985**, *107*, 7198. (e) Nakamura, N.; Kohzuma, T.; Kuma, H; Suzuki, S. *Inorg. Chem.* **1994**, *33*, 1594.

(8) (a) Van der Meer, R. A.; Duine, J. A. *FEBS Lett.* **1988**, *235*, 194. (b) Nagasawa, T.; Yamada, H. *Biochem. Biophys. Res. Commun.* **1981**, *147*, 701. (c) Nagasawa, T.; Yamada, H. *Tib. Tech.* **1989**, *7*, 153.

(9) (a) Minor, W.; Steczko, J.; Bolin, J. T.; Otwinowski, Z.; Axelrod, B. *Biochem.* **1993**, *32*, 6320. (b) Boyington, J. C.; Gaffney, B. J.; Amzel, L. M. *Science* **1993**, *260*, 1482.

(10) (a) Nelson, M. J.; Jin, H.; Turner, I. M., Jr.; Grove, G.; Scarrow, R. C.; Brennan, B. A.; Que, L., Jr. *J. Am. Chem. Soc.* **1991**, *113*, 7072. (b) Jin, H.; Turner, I. M., Jr.; Nelson, M. J.; Gurbiel, R. J.; Doan, P. E.; Hoffman, B. M. *J. Am. Chem. Soc.* **1993**, *115*, 5290.

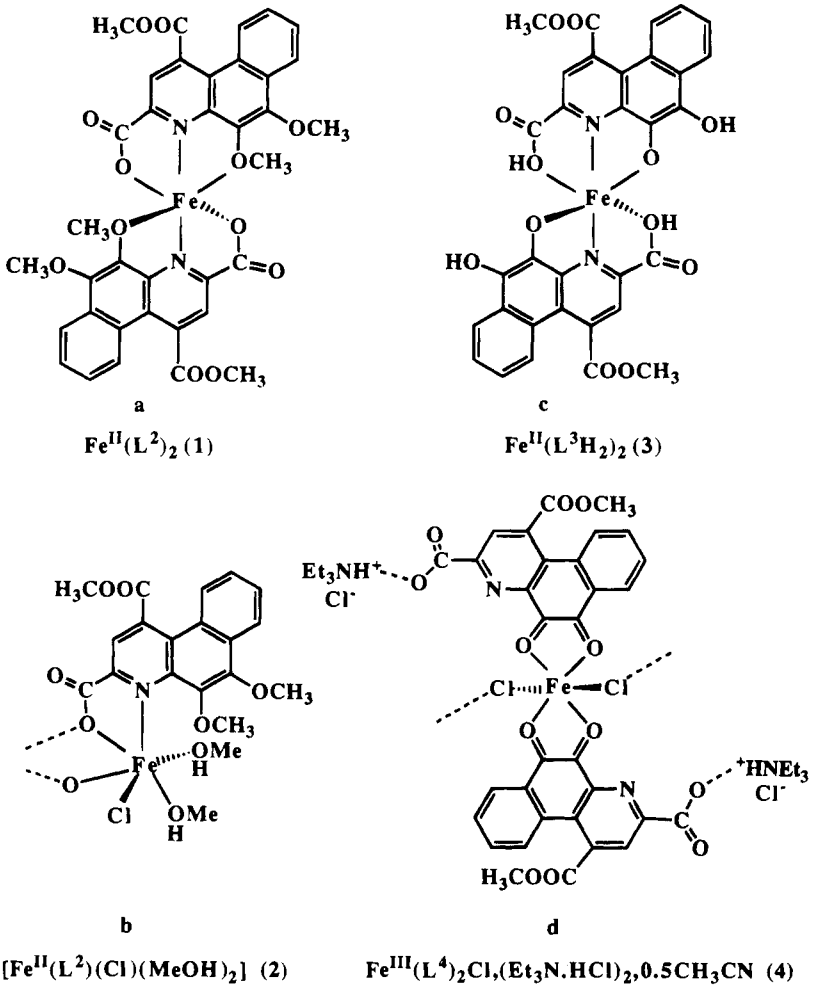

Figure 3. Schematic drawings of the postulated structures for complexes **1** (a), **3** (c), and **4** (d) and of the actual structure for complex **2** (b).

involve stabilization of a C-5 adduct through coordinative activation of the C-5 carbonyl.[6]

In this paper, we report the synthesis of four new analogs of PQQ (L^1H_2, L^2H, L^3H_3, L^4H, Figure 2) and the preparation and IR, Mössbauer, and variable-temperature magnetic susceptibility results for $Fe^{II}(L^2)_2$ (**1**), $[Fe^{II}(L^2)(Cl)(MeOH)_2]_2$ (**2**), $Fe^{II}(L^3H_2)_2$ (**3**), and $Fe^{III}(L^4)_2Cl{\cdot}2(Et_3N{\cdot}HCl){\cdot}0.5CH_3CN$ (**4**) (Figure 3). These are the first reported iron complexes of PQQ analogs. The X-ray crystal structure determination of **2** has been performed, allowing to give a detailed interpretation of its magnetic properties. Finally, a preliminary comparative study of the reaction between L^4H and Fe(II) and Fe(III) is also presented.

Experimental Section

Materials. Ferrous chloride tetrahydrate was purchased from Aldrich, and anhydrous ferric chloride, from Fluka. Iron acetate tetrahydrate was prepared in a Schlenk vessel under an atmosphere of purified nitrogen according to literature methods[11] and stored in an inert atmosphere box (Vacuum Atmospheres H.E.43.2) equipped with a Dri-Train (Jahan EVAC 7). High-grade solvents used for the synthesis of complexes were degassed under vacuum prior to use.

Ligands. 5,6-Dihydroxy-3,4-dihydro-1,3-bis(methoxycarbonyl)-benzo[*f*]quinoline (C). The dimethyl ester of 2-oxo-pent-3-enedioic acid (B) was synthesized by a previously reported method.[12] 3-Amino-1,2-dihydroxy-naphthalene (A) was obtained from freshly prepared *o*-naphthoquinone[13] by a procedure reported in the literature.[14] Compound B (23 g, 0.13 mol) was added at once to a suspension of A (21 g, 0.06 mol) in ethyl acetate (120 mL). The solution became homogeneous and dark red with a slight temperature increase and subsequent formation of a yellow precipitate. Compound C was filtered off after cooling the solution at 2 °C for one night. Yield: 32.3 g (92%). Mp: 220 °C. ^{1}H NMR (δ, ppm, DMSO-d_6): 9.10 (s) and 9.30 (s) (OH); 8.05 (d) and 7.45 (d) (H_7, H_{10}); 7.30 (m, H_8 and H_9); 7.23 (s, NH); 5.80 (m, H_3); 5.25 (m, H_2); 3.80 (s, CH_3); 3.60 (s, CH_3). Anal. Calcd for $C_{17}H_{15}NO_6$: C, 62.05; H, 4.55; N, 4.25. Found: C, 62.43; H, 4.04; N, 4.22. IR (Nujol, cm^{-1}): 1720, 1730 ($\nu_{C=O}$ ester). By chromatography of the filtrate on silica (ethyl acetate/hexane as eluent, 40:60), it was possible to isolate 1.1 g of L^1H_2.

5,6-Dihydroxy-1,3-bis(methoxycarbonyl)benzo[*f*]quinoleine (L^1H_2). Compound C (32.3 g, 0.1 mol) was refluxed in ethyl acetate (150 mL) for 48 h. The solvent was removed under reduced pressure, and the resulting solid was dissolved in ethanol (100 mL). The yellow crystals which formed in the solution were filtered off. Yield: 25.0 g (77%). Mp: 216 °C. ^{1}H NMR (δ, ppm, DMSO-d_6): 10.24 (s) and 9.25 (s) (OH); 8.07 (d) and 8.30 (d) (H_7, H_{10}); 8.12 (s, H_2); 7.61 (t) and 7.75 (t) (H_8, H_9); 4.05 (s, CH_3); 3.98 (s, CH_3). Anal. Calcd for $C_{17}H_{13}NO_6$: C, 62.38; H, 4.00; N, 4.28. Found: C, 62.43; H, 4.04; N, 4.22.

5,6-Dimethoxy-1,3-bis(methoxycarbonyl)benzo[*f*]quinoline (D). An ethereal solution of diazomethane was added to a suspension of the L^1H_2 ligand (1.3 g, 0.004 mol) in methanol (10 mL) until no more nitrogen evolution was observed. After removal of the solvent, flash chromatography (CH_2Cl_2/ether, 90/10) of the residue afforded powdered D which was recrystallized from CH_2Cl_2/CH_3OH. Yield: 1.34 g (95%).

(11) (a) Schreurer-Kestner, M. A. *Bull. Soc. Chim. Fr.* **1863**, *5*, 345. (b) Rhoda, R. N.; Fraioli, A. V. *Inorg. Synth.* **1953**, *4*, 159.
(12) Corey, E. J.; Tramontano, W. H. *J. Am. Chem. Soc.* **1981**, *103*, 5599.
(13) Fieser, L. F. *Organic Synthesis*, J. Wiley: New York, 1943; Coll. Vol. II, p 430.
(14) (a) Stenhouse, J.; Groves, C. E. *J. Chem. Soc.* **1878**, *33*, 415. (b) Greenland, H.; Pinhey, J. T.; Stenhell, S. *Aust. J. Chem.* **1975**, *28*, 2655.

Mp: 138 °C. ^{1}H NMR (δ, ppm, DMSO-d_6): 8.23 (s, H_2); 8.11 (d) and 8.31 (d) (H_7, H_{10}); 7.75 (t) and 7.83 (t) (H_8, H_9); 4.16 (s, CH_3); 4.14 (s, CH_3); 4.13 (s, CH_3); 3.92 (s, CH_3). Anal. Calcd for $C_{19}H_{17}NO_6$: C, 64.22; H, 4.82; N, 3.94. Found: C, 64.32; H, 4.61; N, 4.02. IR (Nujol, cm^{-1}): 1720, 1730 ($\nu_{C=O}$ ester).

3-Carboxy-5,6-dimethoxy-1-(methoxycarbonyl)benzo[*f*]quinoline (L^2H). A 0.1 M solution of NaOH (110 mL) was added dropwise to compound D (3.55 g, 0.01 mol) in dioxane (50 mL), and 15 h later, 200 mL of a satured NaCl solution was added to the mixture. The neutral fraction (75 mg) was extracted with CH_2Cl_2. The aqueous phase was acidified and extracted again with CH_2Cl_2 (100 mL). After removal of the solvent, the yellow residue was crystallized from CH_2Cl_2/CH_3OH to afford pure L^2H. Yield: 3.20 g (90%). Mp: 154 °C. ^{1}H NMR (δ, ppm, DMSO-d_6): 13.60 (s, OH); 8.12 (d) and 8.31 (d) (H_7, H_{10}); 8.20 (s, H_2); 7.74 (t) and 7.82 (t) (H_8, H_9); 4.16 (s, CH_3); 4.14 (s, CH_3); 4.04 (s, CH_3). Anal. Calcd for $C_{18}H_{15}NO_6$: C, 63.34; H, 4.43; N, 4.10. Found: C, 63.46; H, 4.42; N, 4.19.

1,3-Bis(methoxycarbonyl)benzo[*f*]quinoline-5,6-quinone (E). A solution of concentrated nitric acid (0.3 mL) in 3 mL of acetic acid was added dropwise to a suspension of the L^1H_2 ligand (981 mg, 0.003 mol) in acetic acid (5 mL). A precipitate formed immediatly. The reaction mixture was stirred for 1 h, and the product was filtered off, washed with water, and dried. Orange crystals were obtained through crystallization from CH_2Cl_2/CH_3OH. Yield: 910 mg (93%). Mp: 230 °C. ^{1}H NMR (δ, ppm, DMSO-d_6): 8.30 (s, H_2); 7.01 (d) and 8.14 (d) (H_7, H_{10}); 7.67 (t) and 7.72 (t) (H_8, H_9); 4.00 (s, 6H, CH_3). Anal. Calcd for $C_{17}H_{11}NO_6$: C, 62.77; H, 3.41; N, 4.31. Found: C, 62.70; H, 3.35 N, 4.18. IR (Nujol, cm^{-1}): 1720 ($\nu_{C=O}$ ester); 1685 ($\nu_{C=O}$ quinone).

3-Carboxy-1-(methoxycarbonyl)benzo[*f*]quinoline-5,6-quinone (L^4H). A 0.1 M solution of NaOH (33 mL) was added dropwise to a suspension of compound E (975 mg, 0.003 mol) in methanol (20 mL), affording an homogeneous solution. After standing for 12 h, the reaction mixture was extracted with ethyl acetate. The aqueous phase was acidified with dilute hydrochloric acid, and the resulting solution was extracted three times with ethyl acetate (3 × 50 mL). The ethyl acetate extracts were dried over sodium sulfate, filtered, and concentrated. L^4H was finally crystallized from CH_2Cl_2/CH_3OH. Yield: 780 mg (83%). Mp: 238−240 °C. ^{1}H NMR (δ, ppm, DMSO-d_6): 13.81 (s, OH); 8.35 (s, H_2); 7.60 (d) and 8.14 (d) (H_7, H_{10}); 7.67 (t) and 7.81 (t) (H_8, H_9); 3.95 (s, CH_3). Anal. Calcd for $C_{16}H_9NO_6$,H_2O: C, 58.36; H, 3.37; N, 4.25. Found: C, 58.25; H, 3.28; N, 4.31.

3-Carboxy-5,6-dihydroxy-1-(methoxycarbonyl)benzo[*f*]quinoline (L^3H_3). A 0.1 M solution of NaOH (180 mL) was added dropwise to a suspension of L^1H_2 (2.1 g, 0.006 mol) in methanol (50 mL). Following the procedure previously described for the preparation of L^4H, 1.4 g of yellow crystals of L^3H_3 was obtained (yield 70%) after crystallization from CH_2Cl_2/CH_3OH. Mp: 254 °C (dec). ^{1}H NMR (δ, ppm, DMSO-d_6): 13.2 (s, COOH); 10.27 and 9.87 (s, OH); 8.16 (s, H_2); 8.33 (d) and 8.10 (d) (H_7, H_{10}); 7.63 (t) and 7.77 (t) (H_8, H_9); 4.07 (s, CH_3). Anal. Calcd for $C_{16}H_{11}NO_6$: C, 61.30; H, 3.50; N, 4.47. Found: C, 61.31; H, 3.52 N, 4.55.

Complexes. The ferrous complexes were synthetized and stored in an inert-atmosphere box (Vacuum Atmospheres H.E.43.2) equipped with a Dri-Train (Jahan EVAC 7).

$Fe^{II}(L^2)_2$ (1). A solution of iron(II) acetate ($Fe^{II}(CH_3CO_2)_2{\cdot}2H_2O$) (0.48 mmol) in methanol (3 mL) was added dropwise to a suspension of L^2H in methanol (4 mL, 0.91 mmol). A red-purple precipitate formed before the end of iron(II) acetate addition. The resulting slurry was stirred for 72 h at room temperature. The complex was filtered off, washed with methanol, and dried under vacuum for 5 h. Yield: 77%. The same $Fe^{II}(L^2)_2$ complex was obtained regardless of the L^2H/$Fe(AcO)_2$ stoichiometry. Complex **1** can also be obtained from reaction of a methanolic solution of $Fe^{II}Cl_2{\cdot}4H_2O$ with a methanolic solution of L^2Na in the 1:2 stoichiometry. Anal. Calcd for $C_{36}H_{28}N_2O_{12}Fe$: C, 58.7; H, 3.8; N, 3.8; Fe, 7.6. Found: C, 59.0; H, 4.0; N, 3.6; Fe, 7.6.

$[Fe^{II}(L^2)(Cl)(CH_3OH)_2]_2$ (2). L^2H (303 mg, 0.89 mmol) was added to a solution of iron(II) chloride (142 mg, 0.87 mmol) in methanol (15 mL). A brown color developped immediately, and 3 h later, a 0.2 M solution of NaOH was added dropwise to the solution until a precipitate formed. After stirring of the reaction mixture for 72 h, the precipitate was filtered off, washed with methanol, and dried under vacuum for 6 h. Yield: 70%. Complex **2** has also been obtained from the reaction of a methanolic solution of $Fe^{II}Cl_2{\cdot}4H_2O$ with a methanolic solution of L^2Na in the 1:1 stoichiometry. Single crystals of **2** suitable for X-ray studies were obtained by slow concentration of 2×10^{-3} M methanolic solutions of the complex in an inert-atmosphere box. Anal. Calcd for $C_{20}H_{22}NO_8ClFe$: C, 48.4; H, 4.4; N, 2.8; Cl, 7.2; Fe, 11.3. Found: C, 48.2; H, 4.2; N, 2.9; Cl, 7.3; Fe, 11.3.

$Fe^{II}(L^3H_2)_2$ (3). A solution of iron(II) acetate (0.48 mmol) in 1.5 mL of methanol was added dropwise to a suspension of L^3H_3 (0.91 mmol) in methanol (20 mL). A brown precipitate usually formed before the end of iron(II) acetate addition. The slurry was stirred for 72 h at room temperature. The resulting complex was filtered off, washed with methanol, and dried under vacuum for 5 h. Yield: 91%. When the reaction was carried out with iron(II) chloride instead of iron(II) acetate, a brown color developed immediately but no precipitate formed. It was necessary to add a 0.2 M solution of NaOH dropwise to the reaction mixture until precipitation of complex **3**. Anal. Calcd for $C_{32}H_{20}N_2O_{12}Fe$: C, 56.5; H, 3.0; N, 4.1; Fe, 8.2. Found: C, 56.0; H, 3.0; N, 4.1; Fe, 7.9.

$Fe^{III}(L^4)_2Cl{\cdot}2(Et_3N{\cdot}HCl){\cdot}0.5CH_3CN$ (4). A solution of iron(III) chloride (0.70 mmol) in dry acetonitrile (5 mL) was added dropwise to a suspension of L^4H (1.41 mmol) in dry acetonitrile (15 mL). Half an hour later, triethylamine (1.45 mmol) was added to the reaction mixture inducing a color change from orange to dark-green. The solution was stirred for 6 days at room temperature, and freshly distilled diethyl ether was added until a brown precipitate began to form. The reaction mixture was let to stand for 2 days, and the resulting precipitate was filtered off, washed with dry diethyl ether, and dried under vacuum for 5 h. Yield: 58%. Anal. Calcd for $C_{45}H_{49.5}N_{4.5}O_{12}Cl_3Fe$: C, 53.6; H, 5.0; N, 6.3; Cl, 10.6; Fe, 5.5. Found: C, 53.7; H, 6.0; N, 6.2; Cl, 10.0; Fe, 5.5.

Physical Measurements. Melting points were determined with a Kofler block and are given without correction. Element analyses were carried out at the microanalytical laboratory of the Laboratoire de Chimie de Coordination for C, H, and N and at the Service Central de Microanalyses du CNRS in Vernaison for Fe and Cl. IR spectra were recorded on a Perkin-Elmer 983 spectrophotometer coupled with a Perkin-Elmer infrared data station. Samples were run as Nujol mulls for C, D, and E and CsBr pellets prepared under nitrogen in the drybox for all other compounds. NMR spectra were recorded on a Bruker ARX 250 spectrometer, and chemical shifts are given in ppm relative to DMSO as internal reference (2.49 ppm relative to TMS)

Variable-temperature magnetic susceptiblity data were obtained on powdered polycrystalline samples with a Quantum Design MPMS SQUID susceptometer. Diamagnetic corrections were applied by using Pascal's constants. Least-squares computer fittings of the magnetic susceptibility data were accomplished with an adapted version of the function-minimization program STEPT.[15]

X-band powder EPR spectra were obtained on a Bruker ESP 300 E spectrometer with magnetic field modulation at 100 kHz. The microwave frequency was measured with a Racal-Dana frequency meter, and the magnetic field was measured with a Bruker NMR probe gaussmeter. A Bruker liquid-nitrogen cryostat was used for measurements between 300 and 90 K. Powdered samples were loaded in 3 mm cyclindrical quartz tubes in the drybox and then degassed and sealed under vacuum.

Mössbauer measurements were obtained on a constant-acceleration conventional spectrometer with a 25 mCi source of ^{57}Co (Rh matrix). Isomer shift values (δ) throughout the paper are given with respect to metallic iron at room temperature. The absorber was a sample of 120 mg of microcrystalline powder enclosed in a 2 cm diameter cylindrical plastic sample holder, the size of which had been determined to optimize the absorption. Variable-temperature spectra were obtained in the 300−4.2 K range, by using a MD 306 Oxford cryostat, the thermal scanning being monitored by an Oxford ITC4 servocontrol device (±0.1 K accuracy). A least-squares computer program[16] was used to fit the Mössbauer parameters and determine their standard deviations of statistical origin (given in parentheses).

X-ray Crystal Structure Determination. A dark orange platelet (0.50 × 0.40 × 0.20 mm) was coated with vaseline in an inert-

(15) Chandler, J. P. Program 66, Quantum Chemistry Program Exchange, Indiana University, 1973.
(16) Varret, F. *Proceedings of the International Conference on Mössbauer Effect Applications*; *Jaipur, India, 1981*; Indian National Science Academy: New Delhi, 1982.

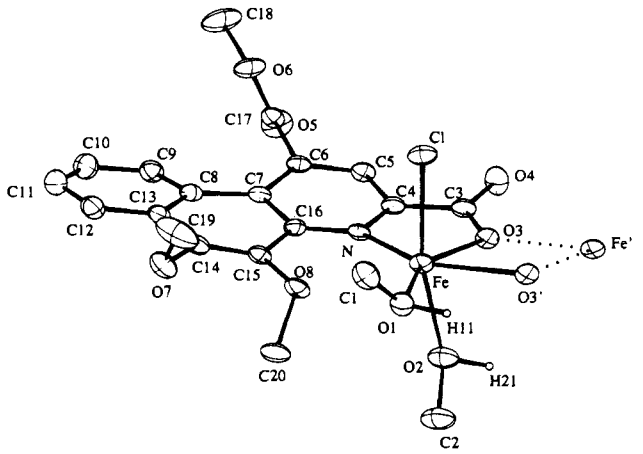

Figure 4. ORTEP view of the $[Fe^{II}(L^2)(Cl)(MeOH)_2]$ (**2**) molecule with atom numbering.

Table 1. Crystallographic Data for $[Fe^{II}(L^2)(Cl)(MeOH)_2]$

chem formula: $FeC_{20}H_{22}NO_8Cl$	fw: 495.7
space group: $P\bar{1}$(No. 2)	$T = 20$ °C
$a = 9.588(6)$ Å	$\alpha = 96.62(5)°$
$b = 10.014(7)$ Å	$\beta = 99.20(5)°$
$c = 11.763(5)$ Å	$\gamma = 107.95(7)°$
$V = 1035(1)$ Å^3	$\lambda = 0.7107$ Å
$\varrho_{calc} = 1.58$ g cm^{-3}	μ(Mo Kα) = 8.95 cm^{-1}
$Z = 2$	transm coeff = 0.922−1.0
$R(\Sigma\|\|F_o\| - \|F_c\|\|)/(\Sigma\|F_o\|) = 0.054$	R_w ($[\Sigma(\|F_o\| - \|F_c\|)^2/(\Sigma\|F_o\|)^2]^{1/2}$) = 0.063

atmosphere box, sealed in a Lindemann capillary, and mounted on an Enraf-Nonius CAD 4 diffractometer. A total of 3867 reflections in four octants (h, $-11 \rightarrow 11$; k, $-11 \rightarrow 11$; l, $0 \rightarrow 13$) with $3 \leq 2\theta \leq 50°$ were collected at 22 °C using Mo Kα radiation with a graphite monochromator ($\lambda = 0.7107$ Å). The crystal of $[Fe^{II}(L^2)(Cl)(MeOH)_2]$ belongs to the triclinic system, and its space group was assigned as $P\bar{1}$ (No. 2). The crystal quality was monitored by scanning three standard reflections every 2 h. No significant variation was observed during the data collection. After corrections for Lorentz and polarization effects, an empirical absorption correction was applied.[17] Cell constants were obtained from a least-squares fit of 25 reflections.

Structure Solution and Refinement. The structure was solved by using direct methods.[18] With a final data set of 2683 reflections ($I > 3\sigma(I)$), all non-hydrogen atoms were located in successive Fourier difference maps and least-squares refinement cycles.[19] The OH hydrogen atoms of the methanol molecules were found on a difference Fourier synthesis and refined while the others were included in calculations with a constrained geometry (C−H = 0.98 Å). Non-hydrogen atoms were refined anisotropically. OH hydrogen atoms of the methanol molecules were refined isotropically. All other hydrogen atoms were coupled to their bonded carbon atom with an isotropic temperature factor 20% higher than that of their bonded atom. The atomic scattering factors and anomalous dispersion terms were taken from the standard compilation.[20] The final full-matrix least-squares refinement converged to $R = 0.054$ and $R_w = 0.063$ with a unit weighting scheme.

All calculations were performed on a PC computer using the programs SHELXS 86[18] and CRYSTALS.[19] The dimeric complex molecule $[Fe^{II}(L^2)(Cl)(MeOH)_2]_2$ is shown in Figure 4 with atom numbering. The crystallographic data are summarized in Table 1. Final fractional atomic coordinates with their estimated standard deviations and selected bond lengths and bond angles are given in Tables 2 and 3, respectively.

(17) Walker, N.; Stuart, D. *Acta Crystallogr., Sect. A: Found. Crystallogr.* **1983**, *A39*, 158.
(18) Sheldrick, G. M. *SHELXS 86, Program for Crystal Structure Solution*, University of Göttingen: Göttingen, Germany, 1986.
(19) Watkin, D. J.; Carruthers, J. R.; Betteridge, P. W. *CRYSTALS, Advanced Crystallographic Program System*, Oxford University: Oxford, U.K., 1988.
(20) Cromer, D. T.; Waber, J. T. *International Tables for X-ray Crystallography*; Kynoch Press: Birmingham, England, 1974; Vol. IV.

Table 2. Fractional Atomic Coordinates (ESD's) and Isotropic Equivalent Temperature Factors for $[Fe^{II}(L^2)(Cl)(MeOH)_2]$

atom	*x/a*	*y/b*	*z/c*	U_{eq} (Å^2)[a]
Fe	0.4390(1)	0.34231(9)	0.88602(8)	0.0268
Cl	0.1793(2)	0.3157(2)	0.8916(2)	0.0398
N	0.4014(5)	0.3967(5)	0.7070(4)	0.0237
O(1)	0.4323(5)	0.1520(4)	0.9468(4)	0.0349
O(2)	0.6859(5)	0.4075(5)	0.9111(4)	0.0464
O(8)	0.3931(5)	0.1318(4)	0.7103(4)	0.0328
O(7)	0.2393(5)	−0.0813(4)	0.5105(4)	0.0414
O(3)	0.4978(4)	0.5700(4)	0.9137(3)	0.0261
O(4)	0.4609(6)	0.7509(4)	0.8332(4)	0.0342
O(6)	0.0815(5)	0.4845(5)	0.3869(4)	0.0392
O(5)	0.2928(6)	0.6471(5)	0.3690(4)	0.0454
C(1)	0.3042(9)	0.0265(7)	0.9271(7)	0.0481
C(2)	0.7857(9)	0.3323(9)	0.9457(8)	0.0568
C(20)	0.5047(8)	0.0609(7)	0.7043(6)	0.0383
C(19)	0.133(1)	−0.1440(8)	0.573(1)	0.0654
C(3)	0.4605(7)	0.6265(6)	0.8260(5)	0.0304
C(4)	0.4106(6)	0.5335(6)	0.7104(5)	0.0281
C(5)	0.3623(7)	0.5832(6)	0.6102(5)	0.0272
C(6)	0.3016(6)	0.4926(6)	0.5072(5)	0.0269
C(7)	0.2978(6)	0.3478(6)	0.4973(5)	0.0258
C(8)	0.2448(6)	0.2456(6)	0.3909(5)	0.0306
C(17)	0.2280(7)	0.5505(6)	0.4109(5)	0.0304
C(9)	0.2161(7)	0.2784(7)	0.2791(5)	0.0366
C(10)	0.1553(8)	0.1748(8)	0.1814(6)	0.0460
C(11)	0.1187(8)	0.0310(8)	0.1911(6)	0.0477
C(12)	0.1542(7)	−0.0045(7)	0.2983(6)	0.0414
C(13)	0.2192(6)	0.0988(6)	0.3981(5)	0.0312
C(14)	0.2651(7)	0.0617(6)	0.5096(6)	0.0327
C(15)	0.3362(7)	0.1607(6)	0.6045(5)	0.0284
C(16)	0.3492(6)	0.3088(6)	0.6037(5)	0.0269
C(18)	−0.0034(9)	0.527(1)	0.2927(8)	0.0570
H(11)	0.469(6)	0.187(6)	1.033(5)	0.03(2)
H(21)	0.76(1)	0.51(1)	0.965(8)	0.11(3)

[a] $U_{eq} = 1/3$ of the trace of the orthogonalized U_{ij} tensor.

Table 3. Selected Interatomic Distances (Å) and Angles (deg) for $[Fe^{II}(L^2)(Cl)(MeOH)_2]$[a]

	Iron Environment		
	Distance		
Fe−Cl	2.433(2)	Fe−O(2)	2.213(5)
Fe−N	2.237(5)	Fe−O(3)	2.145(4)
Fe−O(1)	2.098(4)	Fe−O(3)′	2.329(4)
Fe···Fe′	3.645(4)		
	Angles		
Fe−O(3)−Fe′	109.2(1)	N−Fe−O(1)	133.1(2)
Cl−Fe−O(1)	94.8(1)	N−Fe−O(3)′	145.6(1)
Cl−Fe−O(2)	167.4(1)	O(1)−Fe−O(3)	151.4(2)
Cl−Fe−O(3)	90.8(1)	O(2)−Fe−O(3)	79.2(2)
Cl−Fe−O(3)′	88.6(1)	O(1)−Fe−O(2)	90.5(2)
Cl−Fe−N	89.0(1)	O(1)−Fe−O(3)′	81.2(1)
N−Fe−O(3)	74.9(2)	O(2)−Fe−O(3)′	80.9(2)
N−Fe−O(2)	95.7(2)	O(3)−Fe−O(3)′	70.9(1)
	Hydrogen bonds		
	Distances		
O(2)−H(21)	1.08(9)	O(1)−H(11)	1.00(6)
H(21)···Cl′	2.15(9)	H(11)···O(4)′	1.58(6)
O(2)···Cl′	3.176(5)	O(1)···O(4)′	2.579(6)
	Angles		
O(2)−H(21)···Cl′	157	O(1)−H(11)···O(4)′	175

[a] Symmetry: (′) $1 - x$, $1 - y$, $1 - z$.

Results and Discussion

Synthesis of PQQ Analogs. The pyridine ring has been built by cycloaddition from 3-amino-1,2-dihydroxynaphthalene (A) and the dimethyl ester of 2-oxo-pent-3-ene-dioic acid (B) (Figure 2). Compound A was synthesized from freshly prepared[13] *o*-naphthoquinone by a previously reported procedure,[14] and compound B was obtained by a synthetic sequence already described.[12]

The key step for L^1H_2 synthesis, inspired from that of PQQ by Corey and Tramontano,[12] is a Doebner–Von Miller type condensation[21] of A with B. This reaction led to intermediate C which was dehydrogenated upon heating in refluxing ethyl acetate to give L^1H_2 in good yields. The other ligands, L^2H, L^3H_3, and L^4H, were obtained from L^1H_2 according to the scheme of Figure 2. L^2H resulted from a monosaponification of D (prepared by methylation of L^1H_2 with diazomethane) with 1 equiv of diluted NaOH. Similarly, L^3H_3 was obtained through monosaponification of L^1H_2 with 0.1 M NaOH.

Quinone E was prepared by oxidation of L^1H_2 with a nitric acid/acetic acid mixture at room temperature. Under these acidic conditions, the ester functions of L^1H_2 were not hydrolyzed. L^4H was then prepared by monosaponification of E with diluted NaOH. Interestingly, under these conditions, the quinone ring of E was retained. The regiospecificity of the hydrolysis of E was evidenced by a NOE NMR study of L^4H.

It is noteworthy that the new compounds L^1H_2, L^2H, L^3H_3, and L^4H were obtained with good yields (70–80%). Compound E has been previously described, and our samples exhibited spectral characteristics identical to those already reported.[22]

Composition of the Iron Complexes. Reaction of L^2H with iron(II) acetate resulted in the formation of $Fe^{II}(L^2)_2$ (**1**) regardless of the ligand to metal ratio while its reaction with ferrous chloride depended upon the ligand to metal ratio. When the ligand to iron(II) ratio was ≥2, complex **1** characterized by the 1:2 Fe:L stoichiometry, was obtained. However, when the ligand to iron(II) ratio was lower, complex **2**, $[Fe^{II}(L^2)Cl{\cdot}2CH_3OH]_2$, characterized by the 1:1 Fe:L stoichiometry was obtained. Similarly, reaction of L^3H_3 with iron(II) acetate resulted in the formation of $Fe^{II}(L^3H_2)_2$ (**3**) regardless of the ligand to metal ratio while its reaction with ferrous chloride depended upon the ligand to metal ratio. When the ligand to iron(II) ratio was ≥2, complex **3** characterized by the 1:2 Fe:L stoichiometry was obtained. However, when the ligand to iron(II) ratio was lower, several ferrous species were simultaneously obtained which could not be isolated and characterized. Reaction of L^4H with ferric chloride depended upon the ligand to metal ratio. When the ligand to iron(III) ratio was ≥2, complex **4**, $Fe^{III}(L^4)_2Cl{\cdot}2(Et_3N{\cdot}HCl){\cdot}0.5CH_3CN$, characterized by the 1:2 Fe:L stoichiometry was obtained. However, when the ligand to iron(III) ratio was lower, no definite species could be isolated from the reaction mixtures.

These results clearly indicate that in the presence of an excess of ligand the more stable species is a $Fe^{II}L_2$ complex regardless of the chemical nature of the third potential donor of the ligand (OCH_3 for L^2 in **1** or OH for L^3H_2 in **3**). This is probably because both L^2 and L^3H_2 are able to afford a $O^{-}\frown N\frown O^{-}$ chelating donor set to the iron and consequently an octahedral coordination sphere for the iron when two such ligands are involved (Figure 3a,b). However, when L^2H is reacted with iron(II) chloride in a L:Fe ratio low enough to favor the formation of a $Fe^{II}L$ species, the coordinating ability of Cl^- and MeOH is large enough to allow the formation of $Fe^{II}(L^2)(Cl)(CH_3OH)_2$ which is further stabilized through dimerization as shown by the molecular and crystal structure of **2**. However, when L^3H_3 is reacted with iron(II) chloride in a L:Fe ratio lower than 2:1, the simultaneous presence of the 3-carboxylic acid (or carboxylate, depending upon the pH), 4-pyridine, and 5,6-catecholate functions allows competition between the potentially tridentate site and the catecholate site for coordination to the iron and several ferrous species are simultaneously obtained as shown by Mössbauer spectroscopy.

(21) Doebner, O.; Von Miller, W. *Ber.* **1881**, *14*, 2812.
(22) Itoh, S.; Fukui, Y.; Haranou, S.; Ogino, M.; Komatsu, M.; Ohshiro, Y. *J. Org. Chem.* **1992**, *57*, 4452.

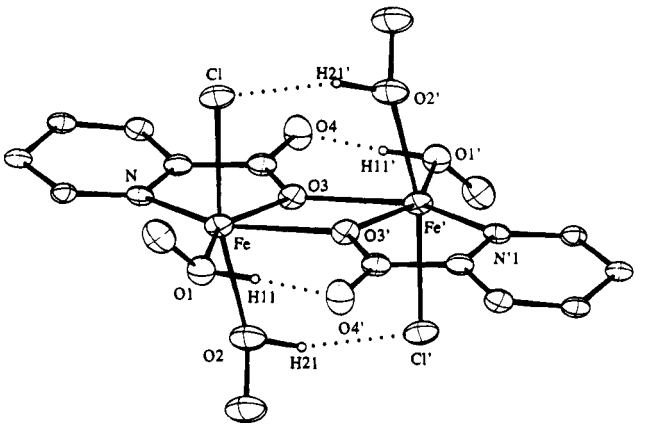

Figure 5. ORTEP view of the carboxylate bridges and hydrogen bonds linking the $[Fe^{II}(L^2)(Cl)(MeOH)_2]$ (**2**) molecules into dimeric units.

Although the $Fe^{III}(L^4)_2Cl{\cdot}2(Et_3N{\cdot}HCl){\cdot}0.5CH_3CN$ formulation of **4** indicates that with an excess of L^4H the more stable species is of the $Fe^{III}L_2$ type, the presence of the quinonic function leads probably to a bidentate coordination mode of the L^4 ligands (Figure 3d) at variance with the tridentate coordination modes of L^2 in **1** and L^3H_2 in **3**, as shown by the IR and magnetic studies.

Molecular Structure of $[Fe^{II}(L^2)(Cl)(CH_3OH)_2]_2$ (2). The complex molecule $Fe^{II}(L^2)(Cl)(CH_3OH)_2$ defining the asymmetric unit (Figure 4) is comprised of one ferrous center, one L^2 ligand coordinated to Fe(II) through its pyridine nitrogen and O(3)-deprotonated carboxylate oxygen atoms, one coordinated chloride anion, and two methanol molecules coordinated to Fe(II) through their oxygen atom. The complex molecules are associated into dimeric units through the O(3) carboxylate oxygen atom of their L^2 ligands and related by an inversion center located at the barycenter of the Fe–O(3)–Fe′–O(3)′ parallelogram (Figure 5). The Fe–O(3)–Fe′ and Fe–O(3)′–Fe′ bridges afford an intradinuclear Fe···Fe′ separation of 3.645(4) Å.

In the asymmetric unit previously described, the six donor atoms afford a distorted octahedral ligand environment for the iron(II). Examination of the Fe–L bond lengths and angles (Table 3) allows us to notice an axial compression of the coordination octahedron along O(1)···O(3). However, due to the departure from 90° of the L–Fe–L angles of the coordination plane defined by O(1), N, O(3), and O(3)′ the symmetry of the coordination octahedron is lower than axial. While the 74.9(2)° value for N–Fe–O(3) can be easily rationalized considering the small bite imposed by the imino–carboxylate chelation mode of L^2, the significant departure from 90° observed for O(3)–Fe–O(3)′ (70.8(1)°), O(1)–Fe–O(3)′ (81.3(1)°), and N–Fe–O(1) (133.1(2)°) results from the peculiar bridging mode of the mononuclear complex molecules to afford dimeric units. The tricyclic L^2 ligands of the two bridged complex molecules are approximately maintained in the Fe–O(3)–Fe′–O(3)′ bridging plane, and four hydrogen bonds are established by the OH groups of the two methanol molecules coordinated to each iron atom (Figure 4 and Table 3). As a result, the constraints resulting from the presence of the O(1)–H···O(4)′ and O(1)′–H···O(4) hydrogen bonds are probably responsible for the departure from 90° of the L–Fe–L angles of the coordination plane defined by O(1), N, O(3), and O(3)′. Similarly, the constraints resulting from the presence of the O(2)–H···Cl′ and O(2)′–H···Cl hydrogen bonds are responsible for the departure from 180° of the O(2)–Fe–Cl angle (167.5(1)°).

In the absence of intermolecular hydrogen contacts and aromatic ring stacking interactions, the crystal packing results

Table 4. Selected Infrared Data (cm^{-1}) for PQQ analogs L^1H_2, L^2H, L^3H_3, and L^4H and Complexes **1**–**4**

	L^1H_2	L^2H	**1**	**2**	L^3H_3	**3**	L^4H	**4**
ν_{OH}(carbox acid)		2681, 2637, 2586			3289, 3245	3320 s, b	3536	
$\nu_{O\cdots{}^+HN}$								3050w, b
ν_{OH}(catechol)	3423, 3315				3444	3320 s, b		
$\nu_{C=O}$(ester)	1728	1734	1732	1740	1730	1725	1730	1735
$\nu_{C=O}$(carbox acid)		1702			1719	1687	1716	
$\nu_{C=O}$(quinone)							1687	1670 b, 1654 b
ν_{COO^-}(as)			1611	1610				1582
ν_{COO^-}(s)			1393	1389				1397
ν_{C-O}(catechol)	1261s, b, 1232				1264, 1224	1435, 1258 s, b		
ν_{C-O}(ether)		1256 s	1264	1263				
		1120	1118	1119				
ν_{CH}(Ph, 4H)	758	757	768, 733	780, 745	747	760, 743	775	794, 749
ν_{Fe-L}			587, 472	589, 477		576, 399		572, 461
			277	279, 226		365, 250		316
ν_{OH}(MeOH)				3495, 3265				
ν_{C-O}(MeOH)				1018				
ν_{NH^+}(Et_3N·HCl)								2627–2500

from van der Vaals interactions between the complex molecules stacked along a direction perpendicular to the [102] plane.

IR Spectroscopy. Table 4 lists some pertinent IR frequencies for the isolated ligands and their iron complexes together with our proposed assignments. L^2H, L^3H_3, and L^4H include a carboxylic acid function characterized by ν_{O-H} absorptions situated at 2681, 2637, and 2586 cm^{-1} for L^2H, 3289 and 3245 cm^{-1} for L^3H_3, and 3536 cm^{-1} for L^4H. These values indicate that the molecules of L^2H are probably associated into dimers through two C−O−H···O=C hydrogen bonds in the solid state, while the carboxylic OH of L^3H_3 is probably involved in a hydrogen bond with the pyridine nitrogen, and the carboxylic OH group of L^4H does not participate in hydrogen contacts.[23] The $\nu_{C=O}$ absorption of the carboxylic acid function observed at 1702, 1719, and 1716 cm^{-1} for L^2H, L^3H_3, and L^4H, respectively, is easily distinguished from the $\nu_{C=O}$ ester absorption situated between 1728 and 1734 cm^{-1} for all four PQQ analogs. The lower $\nu_{C=O}$ carboxylic absorption measured for L^2H (1702 cm^{-1}) indicates the weakening of the double bond and thus confirms the dimerization of this molecule in the solid state which affords a significant conjugation resulting from the involvment of two carboxylic acid functions in an eight-atom C−O−H···O−C−O···H−O ring.[23]

Complexes **1** and **2** include the deprotonated L^2 ligand as indicated by the overall charge balance and the presence of the asymmetric and symmetric ν_{COO^-} carboxylate absorptions and absence of ν_{O-H} and $\nu_{C=O}$ absorptions. The $\Delta = \nu_{as}(CO_2^-) - \nu_s(CO_2^-)$ values (218 and 221 cm^{-1}) measured for **1** and **2**, respectively, clearly indicate that the carboxylates are monodentate in these two complexes.[24] The crystal structure determination confirms the monodentate coordination mode of the carboxylate in **2** and shows that the monodentate carboxylate bridges the iron atoms of the two molecules of a dimeric unit. A similar bridging monodentate mode leading to $\Delta = 240$ cm^{-1} has been evidenced for the acetate anion.[25] In light of the analysis of Deacon and Phillips,[24] both examples indicate that large Δ values reflect large differences in the stretching ability of the C−O$^-$ and C=O bonds, regardless of the number of metal centers coordinated to the monodentate carboxylate. The Δ values for **1** and **2** do not allow one to distinguish between a simple monodentate or bridging monodentate mode concerning the carboxylate in complex **1**, based on IR spectroscopy only. However, comparison of the thermal variation of the magnetic susceptibility of **1** and **2** allows us to conclude that the monodentate carboxylates are not bridging in complex **1** (Magnetic Properties section).

The Ar−O−CH_3 ether functions of L^2H are characterized by the 1256 and 1120 cm^{-1} absorptions in agreement with literature data,[23] and comparison of the IR spectra of L^2H, **1**, and **2** shows that the corresponding C−O−C absorptions occur at similar wavenumbers in the ligand and complexes (1264 and 1118 cm^{-1} (**1**) and 1263 and 1119 cm^{-1} (**2**)). While it is obvious from the crystal structure determination that the ether oxygen atom is not involved in the coordination to the iron center of **2**, it is clear from the Mössbauer study reported in the following section that the iron(II) of complex **1** is in an octahedral ligand environment. Considering the $Fe^{II}(L^2)_2$ formulation of **1** and its magnetic properties, the two L^2 ligands have to be tridentate which requires the involvement of their O-5 ether oxygen atom in the iron coordination sphere (Figure 3a). We are thus led to conclude that the ν_{COC} absorption is not very sensitive to the coordination of the ether oxygen atom to iron in **1**. In other words, it can be considered that the $M-O_{ether}$ bond is very weak as confirmed by contradictory reports concerning the shift of the ν_{COC} absorption upon coordination.[26,27]

Complex **3** includes L^3H_2 deprotonated ligands as indicated by the overall charge balance. Due to their proximity, the carboxylic and catechol ν_{O-H} absorptions cannot be distinguished. However, the presence of the $\nu_{C=O}$ carbonyl absorption and absence of the asymmetric and symmetric ν_{COO^-} carboxylate absorptions clearly evidence that the carboxylic acid function of the ligand is not deprotonated in this complex. Furthermore, the lowering of the carboxylic $\nu_{C=O}$ absorption from 1719 cm^{-1} (L^3H_3) to 1687 cm^{-1} (**3**) indicates the participation of the carboxylic oxygen atom in the iron coordination sphere. The 1264 and 1224 (L^3H_3) and 1435 and 1258 cm^{-1} (**3**) absorptions observed in the IR spectra are attributed to C−O catechol[23] (L^3H_3) and catecholate[28] (**3**) stretches in agreement with previous studies of transition metal complexes with catecholates. They indicate the coordination of one or both catecholate oxygen atoms to the iron. It may thus be concluded that the two L^3H_2 ligands in **3** are coordinated to Fe(II) through their 3-carboxylic acid, N4-pyridine, and deprotonated C5−O$^-$ catechol functions (Figure 3c).

(23) Bellamy, L. J. *The Infrared Spectra of Complex Molecules*, 3rd ed.; Chapman and Hall: New York, 1975; Vol. I.
(24) Deacon, G. B.; Phillips, R. J. *Coord. Chem. Rev.* **1980**, *33*, 227.
(25) Costes, J.-P.; Dahan, F.; Laurent, J.-P. *Inorg Chem.* **1985**, *24*, 1018.
(26) (a) King, A. G.; Taylor, L. T. *Inorg. Nucl. Chem.* **1971**, *33*, 3057. (b) Coleman, W. M.; Boggess, R. K.; Hughes, J. W.; Taylor, L. T. *Inorg Chem.* **1981**, *20*, 1253.
(27) Martinez Lorente, M. A. Doctoral Thesis, *Université Toulouse III*, 1992.
(28) (a) Brown, D. G.; Reinprecht, J. T.; Vogel, G. C. *Inorg. Nucl. Chem. Lett.* **1976**, *12*, 399. (b) Wicklund, P. A.; Brown, D. G. *Inorg. Chem.* **1976**, *15*, 396. (c) Magers, K. D.; Smith, C. G.; Sawyer, D. T. *Inorg. Chem.* **1980**, *19*, 492.

Table 5. Representative Least-squares Fitted Mössbauer Data for Complexes **1**−**4**[a,b]

		complex			
		1	**2**	**3**	**4**
293 K	δ	1.099(3)	1.183(5)	1.059(3)	0.441(3)
	ΔE_Q	2.718(6)	2.503(5)	1.751(6)	1.339(7)
	$\Gamma/2$	0.141(5)	0.131(5)	0.166(4)	0.192(5)
80 K	δ	1.193(1)	1.309(1)	1.197(1)	0.543(4)
	ΔE_Q	3.093(2)	2.874(2)	2.468(2)	1.330(7)
	$\Gamma/2$	0.146(2)	0.143(1)	0.165(2)	0.200(5)
4.3 K	δ	1.217(2)	1.327(1)	1.211(2)	0.548(3)
	ΔE_Q	3.152(3)	2.888(3)	2.534(4)	1.335(5)
	$\Gamma/2$	0.148(2)	0.157(2)	0.172(4)	0.204(4)

[a] δ = isomer shift (mm s^{-1}), ΔE_Q = quadrupole splitting (mm s^{-1}), $\Gamma/2$ = half-width of the lines. [b] Statistical standard deviations are given in parentheses.

The quinone function of L^4H is characterized by the $\nu_{C=O}$ stretching absorption observed at 1687 cm^{-1} as already documented,[29] and the splitting resulting in the presence of two lower absorptions (1680, 1640 cm^{-1}) in complex **4** indicates the involvement of the quinonic group in the coordination to the metal center.[29,30] Complex **4** includes the deprotonated L^4 ligand as indicated by the overall charge balance and presence of the asymmetric and symmetric ν_{COO^-} carboxylate absorptions and absence of the ν_{O-H} and $\nu_{C=O}$ absorptions. The $\Delta = \nu_{as}(CO_2^-) - \nu_s(CO_2^-)$ value of 185 cm^{-1} indicates that the carboxylates are probably ionic in this complex.[24] It may thus be suggested that the carboxylates are not involved in the coordination to the iron and that the two L^4 ligands in **4** are chelated to Fe(III) through their C4 and C5 quinonic oxygen atoms as previously suggested in the case of Ru complexes of PQQ.[31] Furthermore, the simultaneous presence of ν_{NH^+} (2627−2500 cm^{-1}) and $\nu_{O\cdots{}^+HN}$ (3050 cm^{-1}) absorptions and the 1:1 $Et_3N{\cdot}HCl$ to L^4 ratio indicates that each triethylamine hydrochloride molecule is hydrogen bonded to the 3-carboxylate function of one of the L^4 ligands (Figure 3d).

The presence of coordinated methanol in complex **2**, established on the grounds of the elemental analyses and crystal structure determination, is further confirmed by the observation of characteristic OH (3495 and 3265 cm^{-1}) and C−O (1018 cm^{-1}) stretching modes. The observation of two different ν_{O-H} absorptions results from the involvement of the two methanol molecules in hydrogen bonds with different atoms (O(1)−H···O(4)′ and O(2)−H···Cl′).

With the exception of the characteristic benzene ring torsion frequencies observed between 587 and 428 cm^{-1}, it may be assumed that absorptions occuring in the 600−200 cm^{-1} range for complexes **1**−**4** (Table 4) correspond to Fe−L vibrations.

Mössbauer Spectroscopy. The Mössbauer spectra of complexes **1**−**3** recorded at 293, 221, 149, 80, 40, and 4.2 K consist of a single quadrupole split doublet (supplementary material). They were least-squares fitted with Lorentzian lines, and the resulting isomer shift (δ) and quadrupole splitting parameters (ΔE_Q) for selected temperatures are listed in Table 5. The δ and ΔE_Q values clearly indicate the presence of high-spin iron(II) in a distorted octahedral ligand environment for the three complexes. The δ values are weakly temperature dependent due to second-order Doppler shift.[32] The isomer shift values for complexes **1** and **3** are comparable to those of other complexes with N_2O_4 ligand environments. However, they are on the lower side for **3** suggesting an increased covalence of the metal−ligand bond resulting probably from d-electron transfer from the non-σ bonding orbitals of the central atom to the π-acceptor orbitals of corresponding symmetry of the ligand.[33] Such back-donation effects have been observed in ferrous complexes of hydroxy oxime[34] and 3-aminolawsonate[35] ligands which also have a N_2O_4 ligand environment. The larger isomer shift values measured for complex **2** (NO_4Cl ligand environment) are probably related to the presence of the chloride anion.

The low-temperature ΔE_Q values are relatively large indicating that the T_{2g} orbital triplet is split by crystal field distortions affording lower than octahedral symmetry and that the lower state is an orbital singlet. Decrease of ΔE_Q at room temperature indicates the presence of excited T_{2g} levels within thermal reach in these complexes.[36]

The crystal molecular structure of $[Fe^{II}(L^2)(Cl)(CH_3OH)_2]_2$ (**2**) indicates that the distortion of the octahedral geometry is essentially axial and results from a compression along O(1)···O(3) (C_4 axis). Consequently, the ground state must be the $|xy\rangle$ orbital singlet. The 2.89 mm s^{-1} ΔE_Q value at 4.2 K is in agreement with a singlet ground state, and the 2.50−2.87 mm s^{-1} ΔE_Q variation in the 300−80 K temperature range indicates that the energy separation D_s between the singlet ground state and the higher orbital states is small enough to allow thermal population of the higher orbital states at 300 K. It is possible to roughly assess this energy separation assuming that the ΔE_Q slope varies as D_s^{-1}.[37] The slope $d\Delta E_Q/dT$ can be accurately determined by linear regression as -1.87×10^{-3} mm s^{-1} K^{-1} yielding a D_s value of 1280 K. The low-temperature maximum ΔE_Q value is about 25% lower than the maximum value of 4 mm s^{-1} expected for an isolated singlet ground state.[38] This can be attributed to the effect of the spin−orbit interaction. Actually, an axial splitting, D_s, 8−9 times greater than the spin−orbit constant, λ (144 K for the free Fe^{2+} ion[39]), qualitatively explains both the temperature dependence of ΔE_Q and the reduced low-temperature maximum.[36] Although similar comments can be made for complex **1** in view of its ΔE_Q values and their temperature dependence, the nature of the ground state orbital singlet is not known as crystallographic data are not available. However, the similar energy separation between the singlet ground state and higher orbital states (1240 K) indicates a similar D/λ ratio for **1**.

In the case of $Fe^{II}(L^3H_2)_2$ (**3**), the 2.53 mm s^{-1} ΔE_Q value at 4.2 K and its strong temperature dependence indicate that the energy separation between the ground state and the first higher orbital state is small enough to result in a significant thermal population of the latter even at low-temperature. Actually, this energy separation assessed as indicated above is 708 K. For such small orbital level separations, the role of the spin−orbit coupling becomes very important and an understanding of the system would require much more elaborate studies which are beyond the scope of this paper.

(29) (a) Crowley, P. J.; Haendler, H. M. *Inorg Chem.* **1961**, *1*, 904. (b) Berger, S.; Rieker, A. *The Chemistry of the Quinonoid Compounds;* Patai, S. Ed.; John Wiley & Sons: New York, 1974; Vol. 1, Chapter 4.
(30) Garge, P.; Padhye, S.; Tuchagues, J.-P. *Inorg. Chim. Acta* **1989**, *157*, 239.
(31) Schwederski, B.; Kasack, V.; Kaim, W.; Roth, E.; Jordanov, J. *Angew. Chem., Int. Ed. Engl.* **1990**, *29*, 78.
(32) Greenwood, N. N.; Gibbs, T. C. *Mössbauer Spectroscopy;* Chapman and Hall: New York, 1971; Chapter 6.
(33) Vertes, A.; Tarnoczi, T.; Egyed, C. L.; Papp-Molnar, E.; Burger, K. *Acta Chim. Hung.* **1969**, *59*, 19.
(34) Burger, K.; Korecz, L.; Manuaba, I. B. A.; Mag, P. *J. Inorg. Nucl. Chem.* **1966**, *28*, 1673.
(35) Garge, P.; Chikate, R.; Padhye, S.; Savariault, J. M.; De Loth P.; Tuchagues, J. P. *Inorg. Chem.* **1990**, *29*, 3315.
(36) Ingalls, R. *Phys. Rev.* **1964**, *133*, A787.
(37) Ducouret-Cérèze, A.; Varret, F. *J. Phys. (Paris)* **1988**, *49*, 661.
(38) Sams, J. R.; Tsin, T. B. *Inorg. Chem.* **1975**, *14*, 1573.
(39) Trees, R. E. *Phys. Rev.* **1951**, *82*, 683.

Table 6. Effective Magnetic Moment (μ_B) at Selected Temperatures for Complexes **1**–**4**

complex	temp (K)				
	300	100	25	11	2
$Fe^{II}(L^2)_2$ (**1**)	5.13	5.15	5.03	4.77	4.08
$[Fe^{II}(L^2)(Cl)(MeOH)_2]$ (**2**)	4.90	4.67	3.54	2.35	1.07
$Fe^{II}(L^3H_2)_2$ (**3**)	5.28	5.23	4.96	4.54	2.86
$Fe^{III}(L^4)_2Cl{\cdot}2(Et_3N{\cdot}HCl){\cdot}0.5CH_3CN$ (**4**)	4.89	3.81	3.08	2.87	2.41

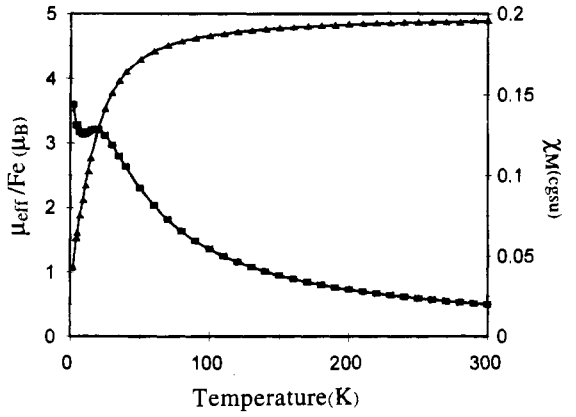

Figure 6. Variable-temperature magnetic susceptibility data for $[Fe^{II}(L^2)(Cl)(MeOH)_2]_2$ (**2**). The solid lines result from a least-squares fit of the data to the theoretical magnetic susceptibility calculated as mentioned in the text.

The Mössbauer spectra of complex **4** recorded at 293, 80, and 4.2 K consist of a single quadrupole split doublet (supplementary material). The δ and ΔE_Q values (Table 5) and the absence of temperature dependence for ΔE_Q[32] are consistent with high-spin iron(III) as further evidenced by the magnetic susceptibility and EPR studies described in the following sections.

Magnetic Properties. The molar magnetic moments of powdered samples of complexes **1**–**4** determined in the 300–2 K temperature range are gathered in Table 6, and the detailed data resulting from the magnetic susceptibility measurements are available in the supplementary material. The effective magnetic moment per iron of **1** and **3** at 300 K is higher than the spin only value of 4.9 μ_B for $S = 2$, as usually observed for high-spin iron(II) complexes. The small dependence of the magnetic moment of complexes **1** and **3** with temperature indicates that they do not experience magnetic exchange interactions. The decrease in their magnetic moment is situated between 25 and 2 K indicating the presence of moderate zero-field splitting of the high-spin iron(II) ground state. These conclusions agree well with the results mentioned in the previous sections leading to their description as isolated mononuclear species in which the iron is surrounded by two tridentate ligands affording a distorted octahedral coordination sphere (Figure 3a,c).

The temperature dependence of the magnetic susceptibility and effective magnetic moment per iron of the Fe(II) dimeric complex **2** are shown in Figure 6. μ_{eff}/Fe decreases from 4.90 μ_B at 300 K to 1.07 μ_B at 2 K, indicating a weak antiferromagnetic coupling of the $S = 2$ spin systems of the two iron(II) ions of each dimeric unit. As previously discussed (X-ray Crystal Structure section), both ligands of the dimeric unit of **2** bridge Fe to Fe′ through the oxygen carboxylate atoms O(3) and O(3′) affording an intradimer Fe···Fe′ separation of 3.645(4) Å. The symmetry related Fe and Fe′ cations are in a distorted octahedral environment with O(1) and O(3) situated at the apices of the compressed octahedron. In the presence of an axial distortion, second-order spin–orbit coupling with the orbital excited states causes the spin quintet to split. With an axial compression the zero-field splitting (ZFS) parameter D is positive while it is negative for an axial elongation.[40] At low-temperature, magnetic susceptibility can distinguish these cases and can be fit to give the value of D which can be as large as 15 cm^{-1} in nearly octahedral ferrous complexes.[41] The exchange coupling constant J is known to range from positive values of a few reciprocal centimeters to values of -15 cm^{-1} for iron(II) complexes.[42]

With this rationale and the experimental results suggesting that the magnetic exchange interactions in **2** are weak, the crystalline field anisotropy and the magnetic exchange interactions are expected to be of the same order of magnitude. Consequently, we attempted to fit the experimental data to the theoretical magnetic susceptibility calculated by exact diagonalization of the effective spin Hamiltonian taking into account single-ion ZFS.[35] The least-squares refinement of the experimental data to the theoretical magnetic susceptibility calculated from this model afforded a very good fit (Figure 6) for the parameters, $J = -2.1$ cm^{-1}, $D = +11.1$ cm^{-1}, $g_\perp = 1.997$, $g_\parallel = 2.029$, and Par = 6%, where Par is the mole percent of a paramagnetic impurity assumed to be a Fe(II) monomer. The absolute value obtained for D indicates that the magnetic behavior of **2** is relevant to the case where the ZFS of the single ion is of the order of magnitude of the exchange integral and cannot be treated as a perturbation. The fact that a reasonable fit could only be obtained for a positive D value is in agreement with the axial compression of the iron ligand environment suggested by the molecular structure of **2**. A subsequent attempt to analyze the variation of the magnetic susceptibility of **2** by employing the expression derived from the isotropic spin-exchange Hamiltonian $\mathcal{H} = -2JS_1S_2$ ($S_1 = S_2 = 2$) and the Van Vleck equation[43] afforded a poorer fit for $J \sim -3$ cm^{-1}, particularly in the low-temperature range. The 6% ratio of paramagnetic component corresponding to the paramagnetic tail observed between 5 and 2 K does not arise from the presence of a ferric impurity as indicated by the magnetic susceptibility and Mössbauer measurements carried out on several samples prepared and protected under an atmosphere of purified nitrogen. While the amount of paramagnetic species is similar for all samples studied with the susceptometer, the Mössbauer spectra do not show any trace of ferric component. Considering the small differences in Mössbauer parameters for **1** and **2**, it can be suggested that this paramagnetic ferrous impurity is complex **1**. Actually, the synthetic procedures leading to complex **2** cannot exclude the simultaneous formation of a very small amount of complex **1**.

The effective magnetic moment per iron of $Fe^{III}(L^4)_2Cl{\cdot}2(Et_3N{\cdot}HCl){\cdot}0.5CH_3CN$ (**4**) at 300 K (4.9 μ_B) is lower than the spin only value of 5.9 μ_B usually observed for high-spin iron(III) complexes ($S = {}^5/_2$). μ_{eff}/Fe decreases regularly from 4.90 μ_B at 300 K to 2.4 μ_B at 2 K, indicating that the metal ions are not magnetically isolated in this ferric species. Although the absence of structural information precludes any interpretation of this antiferromagnetic behavior, it affords information about the possible coordination mode of L^4 in this complex. The presence of magnetic interactions excludes the possibility for

(40) (a) Gill, J. C.; Ivey, P. A. *J. Phys. C.: Solid State Phys.* **1974**, *7*, 1536. (b) Kennedy, B. J.; Murray, K. S. Inorg. Chem. **1985**, *24*, 1552.
(41) (a) Rudowicz, C. *Acta Phys. Pol.* **1975**, *A47*, 305. (b) Champion, P. M.; Sievers, A. J. *J. Chem. Phys.* **1977**, *66*, 1819.
(42) (a) Spiro, C. L.; Lambert, S. L.; Smith, T. J.; Duesler, E. N.; Gagne, R. R.; Hendrickson, D. N. *Inorg. Chem.* **1981**, *20*, 1229. (b) Lambert, S. L.; Hendrickson, D. N. *Inorg. Chem.* **1979**, *18*, 2683. (c) Long, G. L. *Inorg. Chem.* **1978**, *17*, 2702. (d) Tuchagues, J. P.; Hendrickson, D. N. *Inorg. Chem.* **1983**, *22*, 2545. (e) Hartman, J.-A. R.; Rardin, R. L.; Chaudhuri, P.; Phol, K.; Wieghardt, K.; Nuber, B.; Weiss, J.; Papaefthymiou, G. C.; Frankel, R. B.; Lippard, S. J. *J. Am. Chem. Soc.* **1987**, *109*, 7387.
(43) O'Connor, C. J. *Prog. Inorg. Chem.* **1982**, *29*, 203.

L^4 to act as a tridentate ligand through its 3-carboxylic oxygen, 4-pyridine nitrogen, and 5-quinonic oxygen atoms as the iron(III) coordination sphere would then include six donors brought by the two L^4 ligands and result in magnetically isolated ferric ions. The $Fe^{III}(L^4)_2Cl{\cdot}2(Et_3N{\cdot}HCl){\cdot}0.5CH_3CN$ formulation of **4** and its IR spectrum indicate that the L^4 ligands are probably coordinated in a bidentate mode through the quinonic oxygen atoms. In agreement with the magnetic properties of **4**, such a coordination mode would allow intermolecular interactions through bridging ligands occupying the two remaining coordination sites (Figure 3d). In this respect, the Cl^- anions would be good candidates to bridge the $Fe^{III}(L^4)_2$ units into infinite chains and propagate the antiferromagnetic interactions observed. Additional arguments for this hypothesis arise from the 1:1 $Et_3N{\cdot}HCl$ to L^4 ratio and IR evidence that the triethylamine hydrochloride molecules are hydrogen bonded to the 7-carboxylate function of the L^4 ligands.

EPR Spectroscopy. The EPR spectra of complex **4** at 100 and 300 K are similar showing a strong signal at $g = 4.3$ associated with a weaker one at $g = 8.5$ and a broad and weak absorption at $g = 2.02$. This pattern is typical for high-spin iron(III) in a rhombic environment.[44] The weak $g \sim 2$ absorption may be related to the polymeric nature of **4** (see Magnetic Properties section).

Concluding Remarks

The study of the reaction of iron with L^4H and L^3H_3 which contain the quinone (or catechol), pyridine, and carboxylic acid functions of PQQ and L^2H in which the catechol OH groups have been methylated has allowed us to shed some light on the intricate roles played by these functions. In the absence of the quinonic function (L^2H and L^3H_3), the priviledged coordination site is undoubtly the potentially tridentate site including the 3-carboxylic oxygen, 4-pyridine nitrogen, and either the 5-catecholate or 5-methoxy oxygen atoms as shown by the preparation and study of $Fe^{II}(L^2)_2$ (**1**) and $Fe^{II}(L^3H_2)_2$ (**3**). Even when a better donor than the 5-methoxy oxygen of L^2H is available to the iron, this potentially tridentate site is still used but in a bidentate mode as shown by the crystal structure determination of $[Fe^{II}(L^2)(Cl)(MeOH)_2]_2$ (**2**). Of course, in the case of L^2H there is no other coordination site available; however, in the case of L^1H_2 where the 3-COOH site has been esterified and the 5,6-catechol site is available, it has not been possible to obtain any definite species by reaction with ferrous salts, which indicates that the 5,6-catechol function is not a good chelating site in this type of molecule. The same conclusion may be drawn from the reaction of L^3H_3 with iron in a L/M ratio lower than 2 and more or less drastic deprotonation of L^3H_3, as several ferrous species were simultaneously obtained which could not be isolated and characterized.

Also interesting is the ability of the 3-carboxylic oxygen atom to participate in the iron chelation either in its deprotonated (**1** and **2**) or protonated form (**3**). It shall be mentioned at this point that coordination of the protonated 3-carboxylic oxygen atom of L^3H_2 is not only evidenced by the IR spectra of complex **3** but also indirectly confirmed by the inability of L^1H_2 (3-COOH function esterified) to afford any definite species by reaction with Fe(II). It is likely that coordination of the protonated 3-carboxylic oxygen atom is possible in **3** because the 5-catechol site is easily deprotonated, owing to the presence of the adjacent pyridine nitrogen. As a whole, these results show that regardless of its protonation state the 3-carboxylic function is absolutely required for chelation of iron through the tridentate site.

In the presence of the quinonic function (L^4H), the priviledged coordination site is no longer the potentially tridentate $O^{\frown}N^{\frown}O^-$ site but the 5,6-quinonic site as shown by the preparation and study of $Fe^{III}(L^4)_2Cl{\cdot}2(Et_3N{\cdot}HCl){\cdot}0.5CH_3CN$ (**4**). This may result from the smaller size of Fe(III) which would better fit the $O5^{\frown}O6$ bite and/or its higher lewis acidity. The reaction of L^4H with ferrous salts resulted in immediate Fe(II) oxidation with concomitent reduction of the quinonic function of L^4H. The black microcrystalline ferric complex resulting from this reaction could not be identified on the grounds of elemental analysis and IR and Mössbauer spectroscopy, and its insolubility in usual solvents did not allow us to obtain single crystals in order to carry out X-ray diffraction measurements.

While these observations are in agreement with the results showing that Ru^{2+} is chelated at the quinonic site of PQQ,[31] they are at variance with the results of studies concerning other metal ions. Thus, the crystal structure determination of the Ca^{2+} complex of the 2,9-dimethyl ester derivative of PQQ evidences that the metal center is coordinated to the 7-carboxylate oxygen, 6-pyridine nitrogen, and 5-quinonic oxygen atoms constituting the tridentate site.[6] Cu^{2+} cations are chelated at both tridentate sites (O5,N6,O7 and O2,N1,O9) of PQQ in $[Cu_2(PQQ)(terpy)_2]$.[7e] Cd^{2+} is probably chelated at the (O5,N6,O7) tridentate site of PQQ while Na^+ and K^+ can be chelated both at the tridentate and quinonic sites.[7a,b,d] Considering the variety in ionic radius, Lewis acidity, and valence of the studied metal ions, it is difficult to rationalize this ambivalent chelating ability of PQQ and its analogs.

As a final comment, we shall emphasize that this study is the first one involving iron as the metal center and analogs of both the catechol and quinonic forms of PQQ as ligands and affords examples of new chelating modes of PQQ analogs.

Acknowledgment. L.T. thanks the Société de Secours des Amis des Sciences for a doctoral fellowship. J. C. Daran is acknowledged for useful discussions. A. Mari, E. Rivière, and G. Lemercier are acknowledged for their assistance in carrying out the magnetic susceptibility and Mössbauer measurements.

Supplementary Material Available: A listing of complete crystal data and experimental details, a figure showing a view of the unit cell, listings of components of the anisotropic temperature factors, hydrogen atomic positional and thermal parameters, bond lengths and angles, and least-squares planes and deviations of atoms therefrom for complex **2**, figures showing least-squares fitted Mössbauer spectra of complexes **1**–**4**, and listings of detailed data resulting from the magnetic susceptibility measurements for complexes **1**–**4** in the 300–2 K temperature range (24 pages). Ordering information is given on any current masthead page.

IC941294Q

(44) See for example: (a) Ainscough, E. W.; Brodie, A. M.; Plowman, J. E.; Brown, K. L.; Addison, A. W.; Gainsford, A. R. *Inorg. Chem.* **1980**, *19*, 3655. (b) Batra, G.; Mathur, P. *Polyhedron* **1993**, *12*, 2635. (c) Fujii, S.; Ohya-Nishiguchi, H.; Hirota, N.; Nishinaga, A. *Bull. Chem. Soc. Jpn.* **1993**, *66*, 1408.